Crosstalk-free integral imaging display based on double plano-convex micro-lens array

Yazhou Wang (王亚洲)[1], Qionghua Wang (王琼华)[1,2*], Dahai Li (李大海)[1], Huan Deng (邓 欢)[1], and Chenggao Luo (罗成高)[1]

[1]*School of Electronics and Information Engineering, Sichuan University, Chengdu 610065, China*

[2]*State Key Laboratory of Fundamental Science on Synthetic Vision, Sichuan University, Chengdu 610065, China*

[*]*Corresponding author: qhwang@scu.edu.cn*

Received December 31, 2012; accepted February 25, 2013; posted online May 31, 2013

A crosstalk-free integral imaging display consisting of a display panel and double plano-convex micro-lens array is proposed. The double plano-convex micro-lens array includes two micro-lens arrays, A and B. Micro-lens array A is used to eliminate crosstalk by completely reflecting crosstalk lights. Micro-lens array B, located near micro-lens array A, is used to display three-dimensional images. Computer simulations based on ray-tracing are conducted. Crosstalk-free reconstruction images may be clearly observed from the simulation results.

OCIS codes: 110.6880, 100.6890, 110.2990.
doi: 10.3788/COL201311.061101.

Integral imaging (II) is a three-dimensional (3D) display technique first proposed by Lippman in 1908[1]. This technology creates true 3D images in free space that can be seen without special glasses[2−4]. II has been studied by many researchers because of its many characteristics[5,6]. It has continuous viewing points within the viewing angle and provides both vertical and horizontal parallax, unlike lenticular-based stereoscopy. As in holography, natural and realistic 3D images can be displayed in full color. However, low resolution[7,8], limited image depths[9,10], narrow viewing angles[11], and crosstalk[12] limit the development of II. Among these issues, crosstalk is one of the primary disadvantages of II[13].

Generally, in II, each micro-lens has its own corresponding area, i.e., elemental image, on the display panel. Given that the location of each elemental image is restricted, the viewing zone of the viewer is narrow in space. When viewed outside of the viewing zone, a broken 3D image may be observed because the 3D information cannot be completely transmitted by the corresponding micro-lens. Meanwhile, a duplicate 3D image formed by the adjacent micro-lens is reconstructed outside of the viewing zone. Thus, a crosstalk image is observed. 3D images can be reconstructed without crosstalk only if the elemental images have no interference and the lights from each elemental image pass through the corresponding micro-lens in the reconstruction stage. Instead of a micro-lens array in the pickup stage, a sparse camera array can be used to produce a non-interference elemental image array[14]. A field lens and aperture in the pickup stage may be used to avoid interferences among elemental images[15]. In the reconstruction stage, an optical barrier array between the micro-lens and elemental image arrays may be used to prevent the crosstalk of light from adjacent elemental images and considerably eliminate crosstalk[16]. The use of graded-index micro-lens arrays in the reconstruction stage can eliminate crosstalk and avoid pseudoscopic 3D images[17]. A periodic black mask between the elemental image and the micro-lens array can also be used[18].

In this letter, a crosstalk-free II display based on a double plano-convex micro-lens array is proposed. The structure and principle of the proposed display are shown in Fig. 1. The display consists of a display panel and a double plano-convex micro-lens array, which is composed of micro-lens arrays A and B. Micro-lens array A is used to prevent the crosstalk of lights from the non-corresponding micro-lens. For instance, light emanating from point Q in the second elemental image travels through the second micro-lens only and is completely reflected by micro-lenses 1, 3, and 4. Micro-lens array B, located at the right side of micro-lens array A, is used to display 3D images.

The object focal plane of the micro-lens is generally close to the display panel in II. In Fig. 1, l_{F} is the distance between the object focal plane and micro-lens array A, and g is the distance between the display panel and double micro-lens array. The value of g is determined by the parameters of micro-lens array A. When the parameters of micro-lens array B are adjusted, the object focal plane of the double micro-lens array becomes closer to the

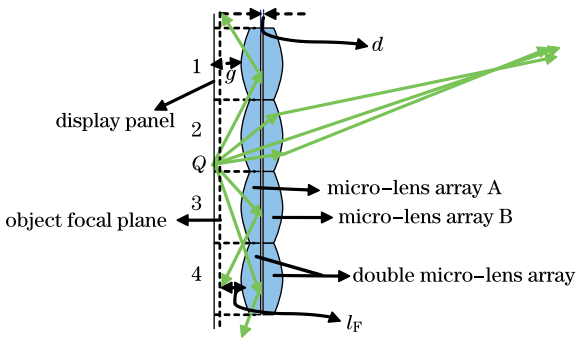

Fig. 1. Structure and principle of the proposed display.

display panel. In other words, the values of $l_{\rm F}$ and g are approximately equal in the proposed display. When $l_{\rm F}$ is greater than g, the 3D image is reconstructed with the real model.

According to lens law, the positions of the principal planes and focal length of the double micro-lens array may be derived from the parameters of the double micro-lens. Consequently, the value of $l_{\rm F}$ can be derived[19]. To calculate the accurate value of $l_{\rm F}$, the thickness of the double micro-lens is considered. The derivation result of $l_{\rm F}$ is shown as

$$l_{\rm F} = \frac{r_1}{n_1 - \frac{n_1 r_1}{M} - 1}, \tag{1}$$

where r_1 and n_1 are the front surface radius and refractive index of micro-lens array A, respectively; M is calculated using

$$M = l_1 + n_1\Big[d + \frac{(l_2 + r_2)n_2 - l_2}{n_2(n_2 - 1)}\Big], \tag{2}$$

where l_1 and l_2 are thicknesses of micro-lens arrays A and B, respectively, r_2 and n_2 are the back surface radius and refractive index of micro-lens array B, respectively, and d is the gap between micro-lens arrays A and B.

To eliminate crosstalk using plano-convex micro-lens array A, the optical characteristics of micro-lens array A must be analyzed. Figure 2 shows the imaging cross-section of a plano-convex micro-lens. The rectangular coordinate system O_1-xy is used. The x-axis is the symmetry axis of the cross-section of the plano-convex micro-lens, and the y-axis coincides with the display panel. Point P is located at the display panel. The coordinates of P and Q_1 are (0, y_1) and (x_2, y_2), respectively. O and R are the center and radius of the front surface, respectively. When $|y_1|$ is greater than $D/2$, the light ray PQ_1 is defined as a crosstalk light ray. Angles θ_1 and θ_2 are the incident and refraction angles of the ray PQ_1 in the front surface, respectively. Angles θ_3 and θ_4 are the incident and refraction angles of the ray Q_1Q_2 in the back surface, respectively. Angle α, which is the angle between OQ_1 and the x-axis, is used to indicate the incident position Q_1 of the light ray PQ_1 in the front surface. The sign of α is determined by

$$\alpha y_2 \geqslant 0. \tag{3}$$

According to Eq. (3), the coordinate of Q_1 can be expressed as $Q_1(R + g - R\cos\alpha,\ R\sin\alpha)$.

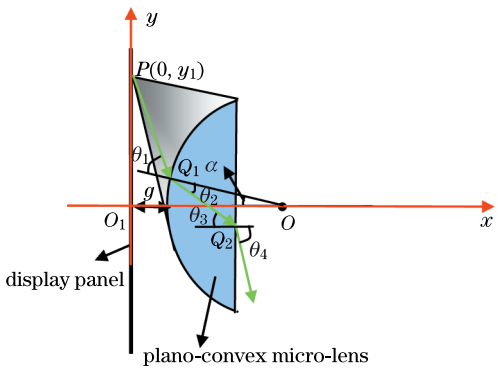

Fig. 2. Imaging cross-section of a plano-convex micro-lens.

When θ_3 is greater than $\arcsin(1/n_1)$, the light ray Q_1Q_2 is completely reflected by the back surface of the plano-convex micro-lens. The following relationship is derived on the basis of geometrical optics.

$$\theta_1(y_1, \alpha) = \arctan\Big(\frac{y_1 - R\sin\alpha}{R\cos\alpha - R - g}\Big) + \alpha, \tag{4}$$

$$\theta_2(y_1, \alpha) = \arcsin\Big(\frac{\sin\theta_1}{n_1}\Big), \tag{5}$$

$$\theta_3(y_1, \alpha) = |\alpha - \theta_2|, \tag{6}$$

$$\theta_4(y_1, \alpha) = \begin{cases} \arcsin(n_1\sin\theta_3) & \theta_3 \leqslant \arcsin\Big(\frac{1}{n_1}\Big) \\ \pi/2 & \theta_3 > \arcsin\Big(\frac{1}{n_1}\Big) \end{cases}. \tag{7}$$

In Eqs. (4)–(7), y_1 and α are derived from θ_1, θ_2, θ_3, and θ_4. The angles α, θ_1, and θ_2 are signed variables, whereas the angles θ_3 and θ_4 are unsigned ones.

According to geometrical relationship, α is limited in the range of $[\alpha_{\min}, \alpha_{\max}]$, which is calculated as

$$\alpha_{\min}(y_1, \alpha) = \max\Big[-\arcsin\Big(\frac{D}{2R}\Big), \beta_1\Big], \tag{8}$$

$$\alpha_{\max}(y_1, \alpha) = \min\Big[\arcsin\Big(\frac{D}{2R}\Big), \beta_2\Big], \tag{9}$$

$$\beta_1(y_1, \alpha) = -\arctan\Big[\frac{g^2 + 2gR}{y_1(g + R) + R\sqrt{y_1^2 + g^2 + 2gR}}\Big], \tag{10}$$

$$\beta_2(y_1, \alpha) = \arctan\Big[\frac{g^2 + 2gR}{y_1(g + R) - R\sqrt{y_1^2 + g^2 + 2gR}}\Big], \tag{11}$$

where D is the pitch of the micro-lens.

According to Fresnel theory[19], when the light ray originating from media a is incident on an interface between media a and media b,the transmittance of the light ray depends on the incident and refraction angles. The transmittance of the light ray can be expressed as

$$T_{\rm s} = \frac{\sin 2\theta_a \sin 2\theta_b}{\sin^2(\theta_a + \theta_b)}, \tag{12}$$

$$T_{\rm p} = \frac{\sin 2\theta_a \sin 2\theta_b}{\sin^2(\theta_a + \theta_b)\cos^2(\theta_a - \theta_b)}, \tag{13}$$

where angles θ_a and θ_b are the incident and refraction angles of the incident light ray, respectively; $T_{\rm s}$ and $T_{\rm p}$ are the transmittances of the s- and p-components, respectively, of the incident light ray. The transmittance of natural lights is the average value of $T_{\rm s}$ and $T_{\rm p}$. According to Eqs. (12) and (13), when PQ_1 travels from the plano-convex micro-lens, the transmittance of the light

ray $P(0,\ y_1)Q_1(R+g-R\cos\alpha,\ R\sin\alpha)$ can be calculated using

$$T(y_1,\ \alpha)=\frac{1}{2}\left[\frac{\sin 2|\theta_1|\times\sin 2|\theta_2|}{\sin^2(|\theta_1|+|\theta_2|)}+\frac{\sin 2|\theta_1|\times\sin 2|\theta_2|}{\sin^2(|\theta_1|+|\theta_2|)\cos^2(|\theta_1|-|\theta_2|)}\right]\times\frac{1}{2}\left[\frac{\sin 2\theta_3\times\sin 2\theta_4}{\sin^2(\theta_3+\theta_4)}+\frac{\sin 2\theta_3\times\sin 2\theta_4}{\sin^2(\theta_3+\theta_4)\cos^2(\theta_3-\theta_4)}\right]. \tag{14}$$

Considering that the angles θ_1 and θ_2 are signed variables, $|\theta_1|$ and $|\theta_2|$ are used in Eq. (14).

Given that the cross-section of the plano-convex micro-lens is symmetric about the x-axis, we only analyze the transmittance of PQ_1 when y_1 is greater than zero. In the proposed display, the crosstalk lights from the range of $y_1 > D/2$ should be eliminated, and the lights from the range of $y_1 < D/2$ should not be completely reflected. Therefore, $P(0,\ D/2)$ should be designed as the critical position of the total reflection. For the light ray PQ_1, which is emitted from $P(0,\ D/2)$, the light ray $Q_1(R+g-R\cos\alpha,\ R\sin\alpha)Q_2$ is completely reflected when satisfing

$$T\left(\frac{D}{2},\alpha\right)=0,\alpha\in\left(\alpha_{\min},\alpha_{\max}\right). \tag{15}$$

Assuming that $\alpha=\alpha_0$ is the unique solution of Eq. (15), Eq. (15) indicates that point $P(0,\ D/2)$ is located at the critical position of the total reflection. On the condition of $y_1 \geqslant D/2$, more and more light rays can be completely reflected with increasing y_1, and the transmittance of crosstalk lights is significantly reduced. Although some of the crosstalk light rays cannot be completely reflected, the luminance of the crosstalk images is reduced and crosstalk-free 3D images are observed. Therefore, the crosstalk in the proposed display is eliminated.

To evaluate the performance of the proposed display, we simulate the reconstruction results of a cross-shaped original object. The height and width of the original object are 120 and 80 mm, respectively. ASAP software is used for the simulation. A double micro-lens array consisting of 50 by 50 micro-lenses is used. The parameters of the display are shown in Table 1.

Figure 3 shows $T-\alpha$ curves with different values of y_1. Curves 1, 2, and 3 represent the transmittance distribution of $y_1=1.49$, 1.50, and 1.51 mm, respectively. The range of α for each curve is calculated with Eqs. (8) and (9). In the range of $\alpha\in(\alpha_{\min},\alpha_{\max})$, curve 2 has a unique crossover point with the x-axis. Therefore, Eq. (15) has a unique solution when the parameters in Table 1 are used. Despite the narrow variation range of y_1, the transmittances exhibit obvious differences among one another (Fig. 3). Therefore, the parameters in Table 1 satisfy the requirements for eliminating crosstalk.

The simulations, which include pickup and reconstruction stages, are performed on the basis of ray-tracing. Firstly, the original object is recorded through the double micro-lens array in the pickup stage, and an elemental image array is produced. Then, a cross-shaped reconstruction image is shown through the double micro-lens array in the reconstruction stage. The shape of the original object is shown in Fig. 4(a). In the simulation, the cross-shaped original object is traced at three depth planes. Three 50×50 elemental image arrays are produced, as shown in Figs. 4(b)–(d). The central depth plane (CDP) is located at a point 109 mm before the micro-lens array.

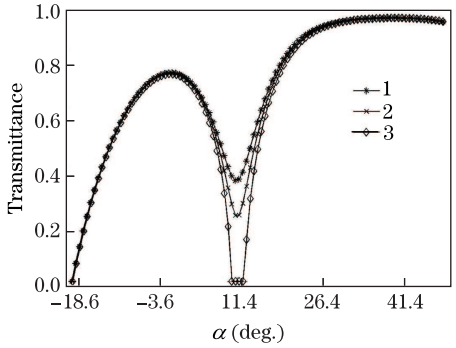

Fig. 3. $T-\alpha$ curves with different values of y_1: (1) 1.49, (2) 1.50, and (3) 1.51 mm.

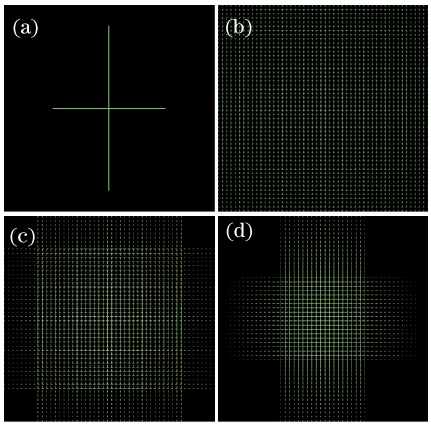

Fig. 4. Original object and elemental image arrays. (a) Shape of the original object. Elemental image arrays recorded in the pickup stage when the original objects are located at points (b) 159, (c) 109, and (d) 59 mm before the double micro-lens array.

Table 1. Parameters of the Proposed Display

Parameter	l_1 (mm)	r_1 (mm)	n_1	l_2 (mm)	r_2 (mm)	n_2	D (mm)	d (mm)	l_F (mm)	g (mm)
Value	2.34	2.0	1.55	2.34	2.0	1.55	3	0.01	0.5202	0.610

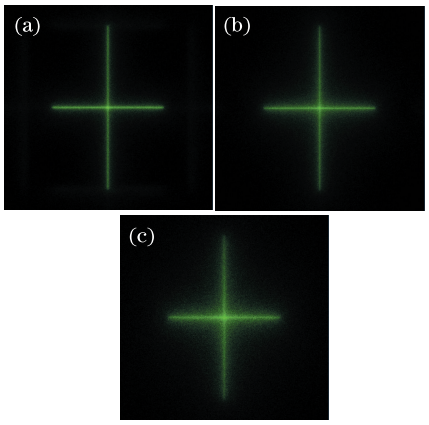

Fig. 5. Crosstalk-free reconstruction images detected (a) 50 mm before the CDP, (b) at the CDP, and (c) 50 mm after the CDP.

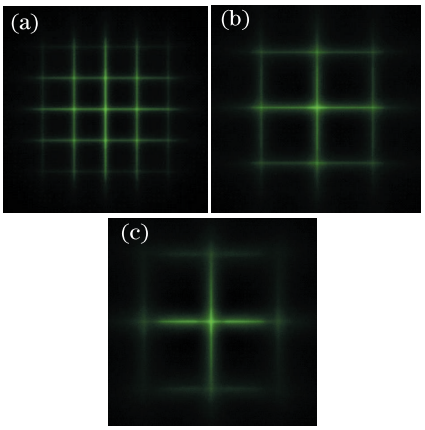

Fig. 6. Conventional reconstruction images detected (a) 50 mm before the CDP, (b) at the CDP, and (c) 50 mm after the CDP.

The reconstruction results of the cross-shaped original object are shown in Fig. 5. Figure 5(a) shows the reconstruction image at a point 50 mm before the CDP. Figure 5(b) shows the reconstruction image at the CDP. Figure 5(c) shows the reconstruction image at a point 50 mm after the CDP. Crosstalk-free reconstruction images are clearly observed at different depth planes. The sizes of all reconstruction images are identical to that of the original object. Compared with the original object, the image quality of all reconstruction images is poorer. Figures 5(a)–(c) show details of the enlarged reconstruction images. Compared with Figs. 5(a) and (c), the reconstruction image in Fig. 5(b) is the clearest. In Figs. 5(a) and (c), the reconstruction images are formed far from the CDP, so the line width of the cross-shaped images is wider and the reconstructed images are more blurred. The reconstruction image in Fig. 5(c) shows numerous stray lights. In comparison, Fig. 6 shows three reconstruction images formed at different depth planes by a conventional II display. Crosstalk images are obviously observed in Figs. 6(a)–(c). Similarly, the reconstruction images in Figs. 6(a) and (c) are blurred because they are formed far from the CDP. Therefore, the proposed display can provide crosstalk-free 3D images.

In conclusion, we present a proposed II display composed of a display panel and double plano-convex micro-lens array consisting of micro-lens arrays A and B. Micro-lens array A is used to eliminate crosstalk. Micro-lens array B, located near micro-lens array A, is used to display 3D images. Compared with conventional displays, the proposed display eliminates crosstalk without requiring additional devices. Simulation results show that the proposed display allows formation of crosstalk-free reconstruction images. The II display has a simple structure and many potential applications.

This work was supported by the National "973" Program of China (No. 2013CB328802), the National Natural Science Foundation of China (Nos. 61036008 and 61225022), and the National "863" Program of China (No. 2012AA011901).

References

1. G. Lippmann, Comptes-Rendus Acad. Sci. **146,** 446 (1908).
2. H. Yoo, Opt. Lett. **36,** 2107 (2011).
3. J. H. Park, K. Hong, and B. Lee, Appl. Opt. **48,** H77 (2009).
4. Q. Wang, *3D Display Technology and Device* (in Chinese) (Science Press, Beijing, 2011).
5. M. C. Forman, N. Davies, and M. McCormick, J. Opt. Soc. Am. A **20,** 411 (2003).
6. M. McCormick and N. Davies, in *Proceedings of the Fourth International Conference on Holographic Systems, Components and Applications* 237 (1993).
7. H. Hoshino, F. Okano, H. Isono, and I. Yuyama, J. Opt. Soc. Am. A **15,** 2069 (1998).
8. T. Ch. Wei, D. H. Shin, and B. G. Lee, J. Opt. Soc. Korea **13,** 139 (2009).
9. C. Luo, Q. Wang, H. Deng, X. Gong, L. Li, and F. Wang, J. Disp. Technol. **8,** 112 (2012).
10. D. Pham, N. Kim, K. Kwon, J. Jung, K. Hong, B. Lee, and J. Park, Opt. Lett. **35,** 3135 (2010).
11. H. Deng, Q. Wang, L. Li, and D. Li, J. Soc. Inf. Disp. **19,** 679 (2011).
12. Y. Kim, J. H. Park, H. Choi, S. Jung, S. W. Min, and B. Lee, Opt. Express **12,** 421 (2004).
13. S. Jung, J. H. Park, H. Choi, and B. Lee, Appl. Opt. **42,** 2513 (2003).
14. H. Deng, Q. Wang, L. Li, and D. Li, Chin. Opt. Lett. **10,** 061102 (2012).
15. K. Yamamoto, T. Mishina, R. Oi, T. Senoh, and M. Okui, J. Opt. Soc. Am. A **26,** 680 (2009).
16. H. Choi, S. W. Min, S. Jung, J. H. Park, and B. Lee, Opt. Express **11,** 927 (2003).
17. J. Arai, F. Okano, H. Hoshino, and I. Yuyama, Appl. Opt. **37,** 2034 (1998).
18. C. Luo, C. Ji, F. Wang, Y. Wang, and Q. Wang, J. Disp. Technol. **8,** 634 (2012).
19. P. W. Hawkes and E. Kasper, *Applied Geometrical Optics* (Academic Press Inc, London, 1989).